McKell Woodland

Department of Mathematics, Brigham Young University, Provo, UT 84602 e-mail: mckell.woodland@rice.edu

Michelle Hsiung

Department of Mathematics, Brigham Young University, Provo, UT 84602 e-mail: mhsiungrussell@byu.net

Erin L. Matheson

Department of Mathematics, Brigham Young University, Provo, UT 84602 e-mail: erin.matheson@du.edu

C. Alex Safsten

Department of Mathematics, Brigham Young University, Provo, UT 84602 e-mail: cas774@psu.edu

Jacob Greenwood

Compliant Mechanisms Research, Department of Mechanical Engineering, Brigham Young University, Provo, UT 84602 e-mail: jacobgreenwood@byu.net

Denise M. Halverson

Department of Mathematics, Brigham Young University, Provo, UT 84602 e-mail: halverson@math.byu.edu

Larry L. Howell

Compliant Mechanisms Research, Department of Mechanical Engineering, Brigham Young University, Provo, UT 84602 e-mail: lhowell@byu.edu

Analysis of the Rigid Motion of a Conical Developable Mechanism

We demonstrate analytically that it is possible to construct a developable mechanism on a cone that has rigid motion. We solve for the paths of rigid motion and analyze the properties of this motion. In particular, we provide an analytical method for predicting the behavior of the mechanism with respect to the conical surface. Moreover, we observe that the conical developable mechanisms specified in this article have motion paths that necessarily contain bifurcation points, which lead to an unbounded array of motion paths in the parameterization plane. [DOI: 10.1115/1.4050294]

Keywords: folding and origami, theoretical kinematics, developable mechanisms

1 Introduction

The basic question that we begin to address in this article is, "Given a developable surface, what types of mechanisms can be constructed on the surface which conform to the surface and have rigid motion?" Rigid motion for such a mechanism means motion without deforming the surface or the links.

Developable surfaces are of interest in design because they can be obtained by bending a flat surface [1], without stretching, tearing, or creasing. In particular, a developable surface is represented mathematically as the image of a smooth path isometry defined on a flat surface. For developable surfaces, the Gaussian curvature, or the product of the two principle curvatures, is necessarily zero [2–4]. Basic families of developable surfaces include planar, cylindrical, conical, and tangent surfaces [2]. Developable surfaces can be represented as the union of a one parameter family of lines in \mathbb{R}^3 , called ruling lines. The existence of ruling lines allows the

Contributed by the Mechanisms and Robotics Committee of ASME for publication in the JOURNAL OF MECHANISMS AND ROBOTICS. Manuscript received September 28, 2020; final manuscript received January 21, 2021; published online March 12, 2021. Assoc. Editor: Philip A. Voglewede.

possibility of creating the mechanisms described in this article by introducing hinges along the ruling lines of the surface.

Engineers can take advantage of the lower production costs and complexity associated with using developable surfaces in their designs. Developable surfaces designed utilizing flexible materials can be manufactured in a flat state and later transformed into their desired curved forms. In addition, developable surfaces can be often manufactured without the heat treatment required for the production of other types of surfaces [5]. Some applications of developable surfaces include steel ship hulls, cartography, architecture, aerostructures, and texture mapping in computer graphics [5–9].

Because developable surfaces are commonly used in design, it is of interest to discover innovative ways to create functionality on these surfaces. One way to increase functionality is to create mechanisms that conform to the surface and are able to achieve motion off of the static surface.

Developable mechanisms are mechanisms that "conform to developable surfaces when both are modeled with zero thickness" [10]. This zero-thickness surface is called the developable mechanism's reference surface [11]. The links of a developable mechanism should not be required to deform for the mechanism to have motion. This can be achieved by aligning hinge lines with the

reference surface's ruling lines [10]. In at least one position, the conformed position, the mechanism's links must conform to the developable reference surface. This requires the rigid links to be shaped to the surface when in their conformed position [11]. Cylindrical developable mechanisms have been discussed in Ref. [11] and have inspired the creation of surgical devices [12]. Since the beginning of this study, additional work has been done on conical developable mechanisms, which are presented in Ref. [13].

The motivation of this article is the demonstration of the mathematical modeling and analysis of developable mechanisms that can be constructed using kirigami techniques, similar to designs for planar surfaces. Kirigami is a variation of origami that includes cutting in addition to folding [14]. Kirigami has inspired the creation of lamina emergent mechanisms, or mechanisms that can be fabricated in a plane, and then emerge from the surface [15]. Although mechanisms on cones are the subject of this article, the planar counterpart can provide an analogy that is helpful for understanding some of the work that follows. The lamina emergent mechanism shown in Fig. 1 is a developable mechanism that is constructed from a planar surface using kirigami and consists of panels linked at hinge joints. As the hinge lines are all parallel, this mechanism will have planar motion. Figure 1(a) shows the mechanism in its as-fabricated state, conforming to a plane. The planar state also represents a bifurcation point (change-point), where the mechanism can change between two different paths depending how it begins to move from this point. These two paths are illustrated in Figs. 1(b)

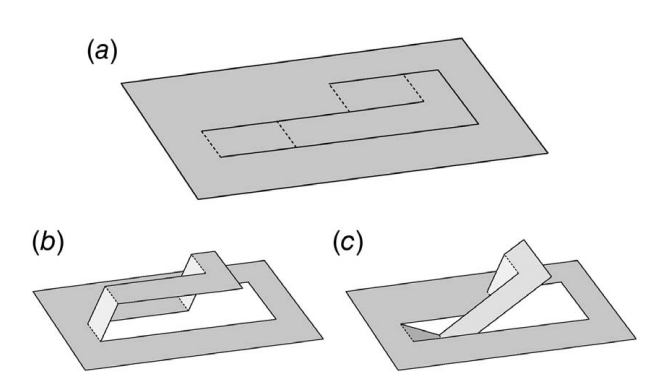


Fig. 1 A lamina emergent mechanism is cut from a single plane of paper and is analogous to the conical developable mechanisms described in this article. (a) The mechanism in its as-fabricated state, which also represents a bifurcation point (change point) where the mechanism can switch between two different motion paths, which are illustrated in (b) and (c).

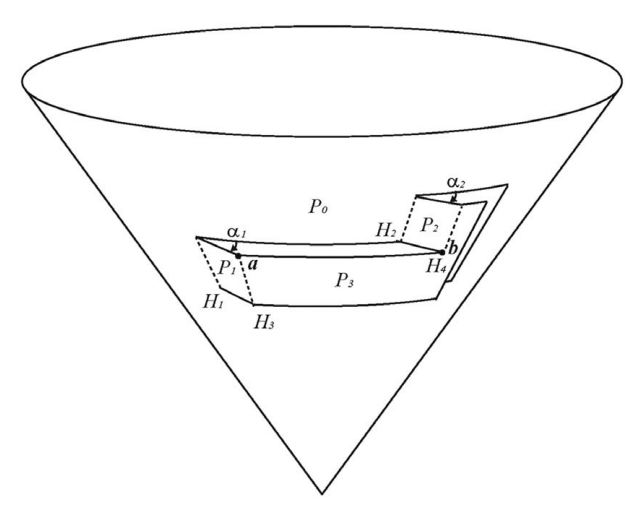


Fig. 2 The conical developable mechanism. Panels P_i , hinges H_i and motion parameters α_i are indicated.

and 1(c). The existence of bifurcation points occurs if the mechanism is a special-case Grashof mechanism [16]. For planar four-bar mechanisms, this depends on link lengths. In the planar case presented in Fig. 1, the opposite links are the same length, making it planar parallelogram linkage, which is a special-case Grashof mechanism. For spherical mechanisms, the Grashof condition is based on link angles [17].

In this article, we construct an analogous mechanism cut out of a cone as shown in Fig. 2. This mechanism will be referred to as a *conical developable mechanism* because it is constructed from a cone. This particular conical developable mechanism is constructed to be a spherical parallelogram linkage, where the link angles of opposite links are equal. This means it is a special-case Grashof mechanism and, if a rigid motion exits, it will necessarily have bifurcation points (change points) [17]. We will proceed by providing a model of the motion of the mechanism and then prove analytically that a rigid motion does exist. We will then provide a detailed description of its motion, with special attention to the initial motion from its conformed position at bifurcation points in the motion path.

2 Construction and Setup

In this section, we detail the construction of the conical developable mechanism and begin to setup the mathematical model utilized in determining the rigid motion of the panels on the mechanism.

2.1 The Mechanism. Let $C \subset \mathbb{R}^3$ be a cone centered on the positive z-axis, with its cone point at the origin, and having cone angle ϕ , i.e. ϕ is the angle between the cone axis and the cone surface. The conical developable mechanism is constructed by cutting out a section of the cone and folding along hinge lines to form three panels (links) with the remainder of the cone forming a panel (a ground link), as shown in Fig. 2. The panel P_0 is the main body of the cone. The panels P_1 and P_2 are joined to the body of the cone along hinge lines, which we will call H_1 and H_2 , respectively. Panel P_3 emerges out of the cone and is connected to panels P_1 and P_2 along hinge lines, which we will call H_3 and H_4 , respectively.

To define P_1 and P_2 and their separation, choose angles δ , $\xi \in (0, 2\pi)$, so that $\delta + \xi < 2\pi$. The angle ξ will be used to determine the length of the panels and the angle δ will be used to determine their separation. Also choose positive numbers z_1 , z_2 , and z_3 with $z_1 < z_2 < z_3$, which will determine the heights of the panels on the cone. Considering \mathbb{R}^3 with cylindrical coordinates (see Fig. 3), the panels P_1 and P_2 are defined by

$$P_1 = \{ (r, \theta, z) \in \mathcal{C}: z_1 < z < z_2, \ 0 < \theta < \delta \}$$

$$P_2 = \{ (r, \theta, z) \in \mathcal{C}: z_2 < z < z_3, \ \xi < \theta < \delta + \xi \}$$

To provide a tab to connect P_3 to P_2 , choose an $\eta > 0$, so that $\delta + \xi + \eta < 2\pi$. The third panel, panel P_3 , which joins P_1 and P_2 is given by

$$\begin{split} P_3 &= \{ (r,\,\theta,\,z) \in \mathcal{C} : z_1 < z < z_2,\, \delta < \theta < \delta + \xi + \eta \} \\ &\quad \cup \, \{ (r,\,\theta,\,z) \in \mathcal{C} : z_2 < z < z_3, \ \delta + \xi < \theta < \delta + \xi + \eta \} \end{split}$$

Note that the edges of P_1 and P_2 in the $z = z_2$ plane are congruent. Likewise, the edges of P_0 and P_3 in the $z = z_2$ plane are congruent.

Viewing the main body of the cone P_0 as fixed, the panels P_1 and P_2 will rotate rigidly about their respective hinge lines H_1 and H_2 . The angle from which the panel P_1 rotates about hinge line H_1 is denoted α_1 , with $\alpha_1 = 0$ corresponding to P_1 being in the conformed position (i.e., being flush with the body of the cone). Similarly, the angle from which the panel P_2 rotates about the hinge line H_2 is denoted as α_2 , with $\alpha_2 = 0$ corresponding to P_2 being in the conformed position. We define the positive direction of the angle to correspond to an initial outward movement. Thus, α_i is the angle between the normal vectors to the panel P_0 and the rotated panel P_i at any point of the intersection of P_0 and P_i . We desire to find a relationship between α_1 and α_2 , so that we can ensure that the rigid motion of panels P_1 and P_2 will admit a rigid motion for P_3 , so that P_3 remains joined to P_1 and P_2 along the hinge lines H_3 and H_4 .

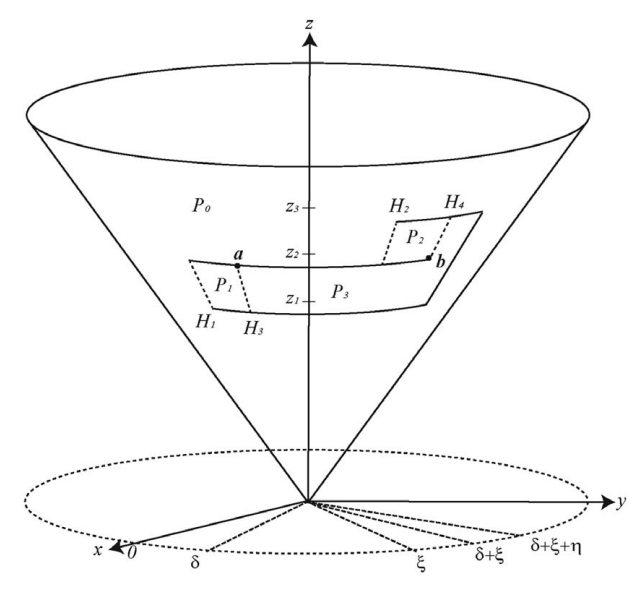


Fig. 3 The design of the conical developable mechanism in the conformed position for $\delta > \xi$. The angle between the z-axis and the cone surface is ϕ .

The panel P_0 , and therefore the hinge lines H_1 and H_2 , are held fixed. Because the position of panel P_1 in \mathbb{R}^3 depends on α_1 , we refer to the image of P_1 in \mathbb{R}^3 resulting from a rotation of α_1 as $P_1[\alpha_1]$. The image of P_2 resulting from a rotation of α_2 is denoted as $P_2[\alpha_2]$. Similarly, the image of the hinge lines H_3 and H_4 in \mathbb{R}^3 , with respect to the angles on which they depend, will be denoted $H_3[\alpha_1]$ and $H_4[\alpha_2]$, respectively. The dependence of a possible position for P_3 on α_1 and α_2 is what is in question.

We can now clearly see that the conical developable mechanism (termed for the type of surface from which it is constructed) behaves kinematically like a spherical mechanism (termed for the existence of a point of concurrence of the hinge lines). A spherical mechanism consists of bars linked at hinge joints whose hinge lines all intersect at a point. The conical reference surface has ruling lines that meet at the cone point (or apex of the cone). A necessary, although not sufficient, condition for a conical developable mechanism to have rigid motion is that the hinges are constructed along straight lines. Thus, the hinges must be constructed along ruling lines. Since P_0 is fixed, any rigid motion of panels P_1 and P_2 maintain that all four hinge lines meet at the cone point throughout the motion. Thus, the mechanism must be a spherical mechanism centered about the cone point (see also Ref. [13]). Methods traditionally used for analyzing spherical mechanisms [18] could also be used in the analysis that follows, but the mathematical approach used here is helpful for the particular analysis and the resulting theorems.

2.2 Defining Points. Consider the following two points on the undeflected mechanism given in cylindrical coordinates:

$$\mathbf{a} = [z_2 \tan \phi, \, \delta, \, z_2]$$
$$\mathbf{b} = [z_2 \tan \phi, \, \delta + \xi, \, z_2]$$

Note that these two points lie on the hinge lines $H_3[0]$ and $H_4[0]$. Indeed, we will be interested in the points $\bf a$ and $\bf b$ as they rotate with the panels $P_1[\alpha_1]$ and $P_2[\alpha_2]$. We denote these rotated points by $\bf a[\alpha_1]$ and $\bf b[\alpha_2]$, respectively.

Converting to Cartesian coordinates, the points $\mathbf{a}[0]$ and $\mathbf{b}[0]$ are represented as follows:

$$\mathbf{a} = \langle z_2 \tan \phi \cos \delta, z_2 \tan \phi \sin \delta, z_2 \rangle \tag{1}$$

$$\mathbf{b} = \langle z_2 \tan \phi \cos(\delta + \xi), z_2 \tan \phi \sin(\delta + \xi), z_2 \rangle$$
 (2)

- **2.3 Motion via Linear Transformation.** The motion of a panel about a hinge line H_i , for i = 1, 2, can be described through a series of linear transformations. The composition of the following transformations will provide the transformations that describe the motion of panel P_i , so that we can determine $P_i[\alpha_i]$:
 - (1) The first transformation moves hinge line H_i to the xz-plane by a clockwise rotation by an angle ω about the z-axis:

$$A_0(\omega) = \begin{pmatrix} \cos \omega & \sin \omega & 0 \\ -\sin \omega & \cos \omega & 0 \\ 0 & 0 & 1 \end{pmatrix}$$
 (3)

(2) Next, we move the image of hinge line H_i to the z-axis by a clockwise rotation of the cone angle ϕ about the y-axis:

$$A_1(\phi) = \begin{pmatrix} \cos \phi & 0 & -\sin \phi \\ 0 & 1 & 0 \\ \sin \phi & 0 & \cos \phi \end{pmatrix} \tag{4}$$

(3) This next rotation about the *z*-axis by an angle α_i is the key transformation. Having applied the transformations $A_0(\omega)$ and $A_1(\phi)$, the image of the hinge line H_i now lies on the *z*-axis. Hence, the rotation of panel P_i about the hinge line H_i at this step is realized by

$$A_2(\alpha_i) = \begin{pmatrix} \cos \alpha_i & \sin \alpha_i & 0 \\ -\sin \alpha_i & \cos \alpha_i & 0 \\ 0 & 0 & 1 \end{pmatrix}$$
 (5)

(4) The transformation $A_1(-\phi)$ reverses the action of $A_1(\phi)$:

$$A_1(-\phi) = \begin{pmatrix} \cos \phi & 0 & \sin \phi \\ 0 & 1 & 0 \\ -\sin \phi & 0 & \cos \phi \end{pmatrix} \tag{6}$$

(5) Finally, the transformation $A_0(-\omega)$ reverses the action of $A_0(\omega)$:

$$A_0(-\omega) = \begin{pmatrix} \cos \omega & -\sin \omega & 0\\ \sin \omega & \cos \omega & 0\\ 0 & 0 & 1 \end{pmatrix}$$
 (7)

We assume that the cone is initially positioned so that $\omega = 0$ for H_1 and $\omega = \xi$ for H_2 (i.e., the mechanism is in its conformed position). Composing the above transformations, we define

$$T_1(\alpha_1) = A_0(0)A_1(-\phi)A_2(\alpha_1)A_1(\phi)A_0(0)$$
(8)

$$T_2(\alpha_2) = A_0(-\xi)A_1(-\phi)A_2(\alpha_2)A_1(\phi)A_0(\xi)$$
(9)

Notice that in the definitions of $T_1(\alpha_1)$ and $T_2(\alpha_2)$, we chose the arguments of A_0 to coincide with the azimuth angle of the hinge lines H_1 and H_2 in cylindrical coordinates. Therefore, $T_i(\alpha_i)$ applied to any point has the effect of rotating that point about the hinge line H_i for i=1, 2. Thus, it is simple to define the motion of the panels P_1 and P_2 about their hinge lines:

$$P_1[\alpha_1] = T_1(\alpha_1)P_1[0]$$

 $P_2[\alpha_2] = T_2(\alpha_2)P_2[0]$

Since $\mathbf{a}[\alpha_1]$ is a point of $P_1[\alpha_1]$ and $\mathbf{b}[\alpha_2]$ is a point of $P_2[\alpha_2]$, we can write:

$$\mathbf{a}[\alpha_1] = T_1(\alpha_1)\mathbf{a}[0] \tag{10}$$

$$\mathbf{b}[\alpha_2] = T_2(\alpha_2)\mathbf{b}[0] \tag{11}$$

3 Rigid Motion

For the conical developable mechanism to have rigid motion, panels P_1 and P_2 must move by a rotation about their hinge lines H_1 and H_2 , respectively. Our goal is to find an open interval U of the real line containing 0 and a function $f:U\to\mathbb{R}$, so that the rigid motion of panels P_1 and P_2 given by $P_1[\alpha_1]$ and $P_2[f(\alpha_1)]$ admits a rigid motion for P_3 as well.

Supposing that such a function f exists, a necessary condition for a rigid motion on panel P_3 is that the distance between points $\mathbf{a}[\alpha_1]$ and $\mathbf{b}[f(\alpha_1)]$ remains constant as α_1 varies. In fact, as we shall see from the rigidity theorem in the next section, this condition is both necessary and sufficient.

Our strategy, therefore, will be to examine the level sets of the function $D:\mathbb{R}^2 \to \mathbb{R}$ defined by

$$D(\alpha_1, \alpha_2) = \|\mathbf{a}[\alpha_1] - \mathbf{b}[\alpha_2]\|^2 \tag{12}$$

where $\mathbf{a}[\alpha_1]$ and $\mathbf{b}[\alpha_2]$ are given by Eqs. (10) and (11), which reference Eqs. (1), (2), (8), (9), and then Eqs. (1)–(7). Then, D represents the square of the standard Euclidean norm between $\mathbf{a}[\alpha_1]$ and $\mathbf{b}[\alpha_2]$.

Note that $D(\alpha_1, \alpha_2)$ is dependent on the design parameters ϕ, δ, ξ , and z_2 . However, it is sufficient for our analysis to set $z_2 = 1$. This is the case because although z_2 modifies the magnitude of the function D, it does not affect the D(0, 0)-level set, which determines possible motion paths. In other words, the movement of two mechanisms with the same design parameters, except the z_i values (i = 1, 2, 3), are exactly the same.

We will find that variations of the design parameters ϕ , δ , and ξ do change the D(0, 0)-level set and may significantly modify the general behavior of the mechanism. When needed to facilitate the discussion of the analysis of the function, we extend the notation of $D(\alpha_1, \alpha_2)$ to

$$D[\phi, \delta, \xi](\alpha_1, \alpha_2)$$

When we use the notation $D(\alpha_1, \alpha_2)$, we assume the values for ϕ , δ ,

The reader may note that the explicit formulas for Eqs. (8)–(12)become quite lengthy and challenging to analyze. Thus, we first verify the existence of a rigid motion by a theoretical analysis. We then demonstrate how to evaluate a rigid motion path computationally.

3.1 Existence of a Rigid Motion. First, we will prove that there exists an open interval U of the real line containing 0 and a function $f:U\to\mathbb{R}$, so that f(0)=0 and $D(\alpha_1, f(\alpha_1))$ is constant. The reasoning here is quite easy, as we will appeal to the implicit function theorem. The explicit form of $D(\alpha_1, \alpha_2)$ is lengthy, but the gradient at the origin is given by

$$\nabla D(0, 0) = \begin{pmatrix} 8z_2^2 \sin\frac{\xi}{2}\sin\phi\tan\phi\sin\frac{\delta}{2}\sin\left(\frac{\delta+\xi}{2}\right) \\ 4z_2^2 \sin\frac{\xi}{2}\sin\phi\tan\phi\left(\cos\left(\delta+\frac{\xi}{2}\right) - \cos\left(\frac{\xi}{2}\right)\right) \end{pmatrix}$$

To apply the implicit function theorem, we must guarantee that $\nabla D(0,0) \neq (0,0)$. Both components of $\nabla D(0,0)$ are a product of several factors. We will simply show that all factors are nonzero. Note that:

- $z_2 \neq 0$ because we chose it to be positive.
- Since 0 < ξ < 2π, we have sin ^ξ/₂ ≠ 0.
 Since 0 < φ < π/2, we have sin φ ≠ 0 and tan φ ≠ 0.
- · Showing that

$$\cos\left(\delta + \frac{\xi}{2}\right) - \cos\frac{\xi}{2} \neq 0$$

requires some work. We will prove by contradiction. Supposing that equality holds and applying the angle addition formula for cosine gives us

$$\cos \delta \cos \frac{\xi}{2} - \sin \delta \sin \frac{\xi}{2} - \cos \frac{\xi}{2} = 0$$

Rearranging terms gives us

$$\frac{\cos \delta - 1}{\sin \delta} = \tan \frac{\xi}{2}$$

Applying the half angle identity for tangent, we are left with

$$\tan\left(-\frac{\delta}{2}\right) = \tan\frac{\xi}{2}$$

This means that $\frac{\delta}{2} + \frac{\xi}{2} = n\pi$ for some integer *n*, or

But we have chosen ξ and δ , so that $0 < \xi + \delta < 2\pi$. So this is a contradiction. Thus,

$$\cos\left(\delta + \frac{\xi}{2}\right) - \cos\frac{\xi}{2} \neq 0$$

Since none of the factors in the second component of $\nabla D(0, 0)$ are equal to zero,

$$\nabla D(0, 0) \neq (0, 0)$$

The implicit function theorem tells us that there is an open interval $U \subset \mathbb{R}$ containing 0 and a function $f:U \to \mathbb{R}$, so that f(0) = 0, and $D(\alpha_1, f(\alpha_1))$ is constant for all $\alpha_1 \in U$. We can now conclude that there exists some rigid motion of the mechanism.

3.2 Solving for the Motion Path. Because of its nonconstructive nature, the implicit function theorem does not specify the rigid motion. However, the rigid motion can be described by a level set that is determined explicitly as the solution to a differential equation. For the purposes of setting up and solving this differential equation, we will write both α_1 and α_2 as functions of another parameter t and use the function $\mathbf{r}:\mathbb{R}\to\mathbb{R}^2$ defined by

$$\mathbf{r}(t) = (\alpha_1(t), \, \alpha_2(t))$$

The differential equation whose solution traces out the level curve is the so-called gradient equation. It is given by

$$\nabla D(\alpha_1, \alpha_2) \cdot \mathbf{r}'(t) = 0$$

with the initial value

$$\mathbf{r}(0) = (0, 0)$$

This is a nonlinear ordinary differential equation, which is underdetermined because we have just one equation with two unknown functions, $\alpha_1(t)$ and $\alpha_2(t)$. We can remedy this by setting:

$$\alpha_1(t) = t$$

Thus, we are left to solve

$$D_{\alpha_1}(t, \alpha_2(t)) + D_{\alpha_2}(t, \alpha_2(t))\alpha_2'(t) = 0$$

or

$$\alpha_2'(t) = -\frac{D_{\alpha_1}(t, \, \alpha_2(t))}{D_{\alpha_2}(t, \, \alpha_2(t))} \tag{13}$$

Equation (13) can be expanded by referencing Eq. (12), substituting in the explicit forms of Eqs. (10) and (11) and taking the appropriate partial derivatives. However, the expanded form is quite lengthy, so we leave it in a symbolic form.

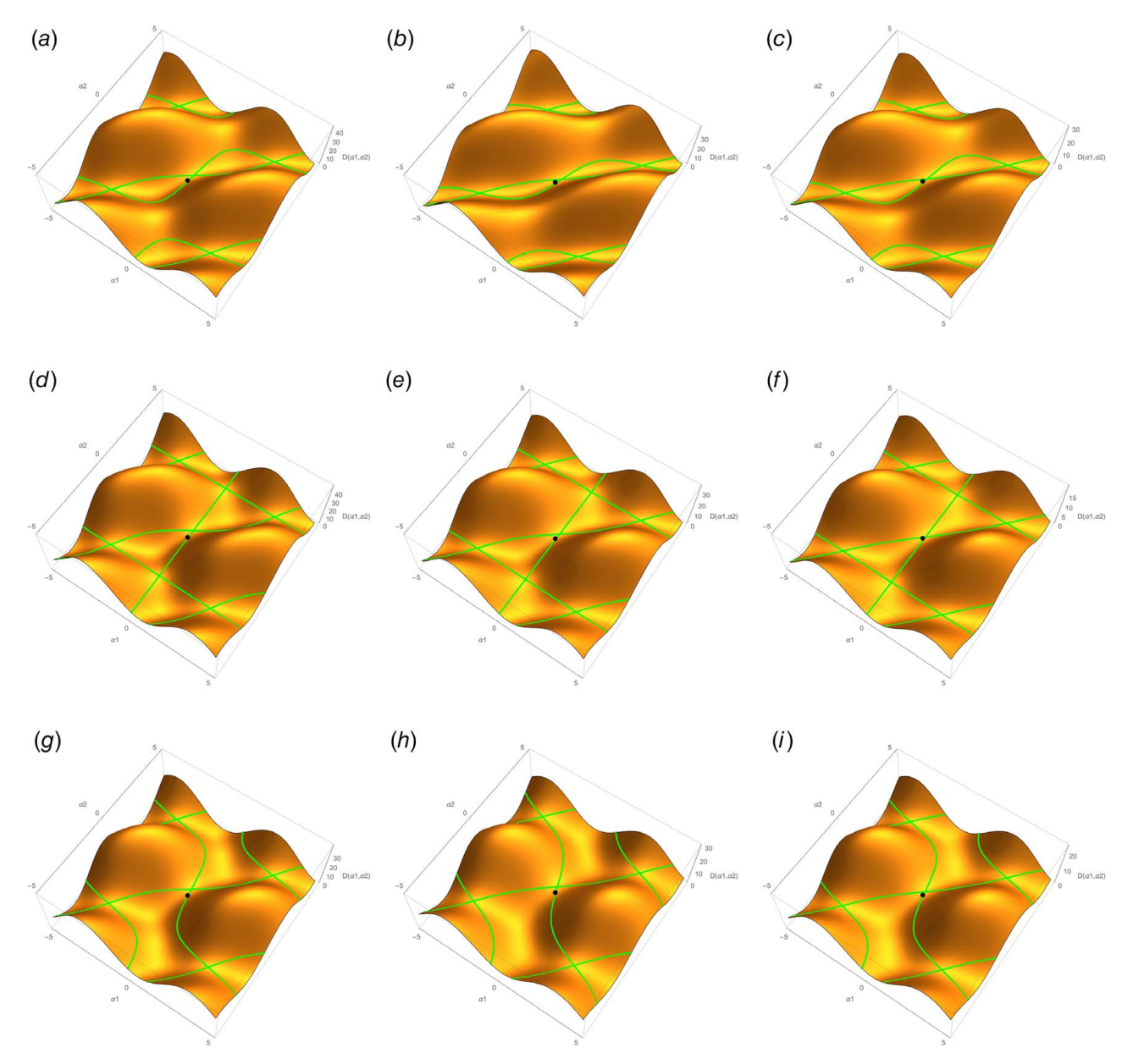


Fig. 4 Plots of the function $D(\alpha_1, \alpha_2)$ for $\phi = \pi/3$ and differing δ and ξ values. The level curves $D(\alpha_1, \alpha_2) = D(0, 0)$ are also indicated. (a) $\delta = \pi/3$, $\xi = \pi/4$, $\phi = \pi/3$, (b) $\delta = \pi/3$, $\xi = \pi/6$, $\phi = \pi/3$, (c) $\delta = \pi/4$, $\xi = \pi/6$, $\phi = \pi/3$, (d) $\delta = \pi/3$, $\xi = \pi/3$, $\phi = \pi/3$, (e) $\delta = \pi/4$, $\xi = \pi/4$, $\phi = \pi/3$, (f) $\delta = \pi/6$, $\xi = \pi/6$, $\phi = \pi/3$, (g) $\delta = \pi/4$, $\xi = \pi/3$, $\phi = \pi/3$, (h) $\delta = \pi/6$, $\xi = \pi/3$, $\phi = \pi/3$, and (i) $\delta = \pi/6$, $\xi = \pi/4$, $\phi = \pi/3$.

We illustrate graphs of the $D(\alpha_1, \alpha_2)$ for several variations of the design parameters δ , ξ , and ψ in Fig. 4. Note that D(0,0) is the functional value of D when the conical developable mechanism is in its conformed position. The curves indicated within the graphs are the D(0,0)-level curves (i.e., the set of points for which $D(\alpha_1,\alpha_2)=D(0,0)$) and are obtained by numerically solving the differential equation Eq. (13) for $\alpha_2(t)$ and then plotting the collection of points $(t,\alpha_2(t))$.

As illustrated in Fig. 5, there are multiple possible paths that are connected to the origin. In Sec. 3.3, we verify that these parameter functions are sufficient to define a rigid motion. It is clear that the relationship between the parameter functions α_1 and α_2 is necessary. An animation of how panels move on these paths is given online.

3.3 The Rigid Transformation. In this section, we define the rigid motion that acts on the developable conical four-bar mechanism. The rigid motion $T:\mathbb{R}^3\times\mathbb{R}\to\mathbb{R}^3$ is piecewise defined as follows:

Recall that $T_1(t)$, $T_2(t)$, **a**, and **b** are defined in Sec. 2 by Eqs. (1), (2), (8), and (9). We define T to be

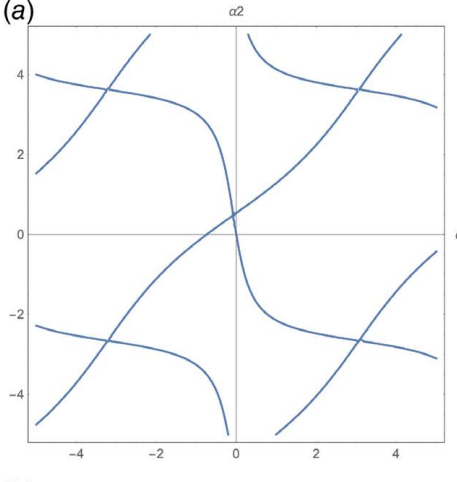
$$T(t)\mathbf{x} = \begin{cases} \mathbf{x}, & \text{if } \mathbf{x} \in P_0 \\ T_1^*(t)\mathbf{x}, & \text{if } \mathbf{x} \in P_1 \\ T_2^*(t)\mathbf{x}, & \text{if } \mathbf{x} \in P_2 \\ T_3^*(t)\mathbf{x}, & \text{if } \mathbf{x} \in P_3 \end{cases}$$
(14)

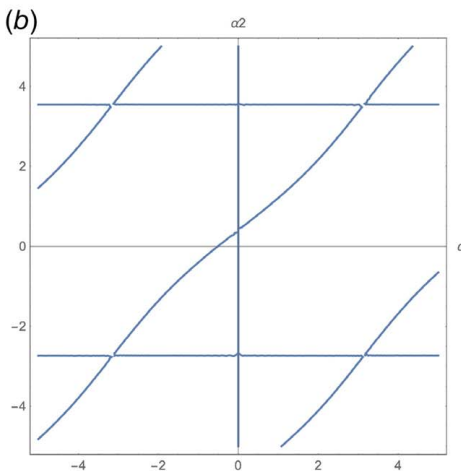
where

$$T_1^*(t) = T_1(t)$$
 and $T_2^*(t) = T_2(\alpha(t))$.

To define $T_3^*(t)$, let $\mathbf{c} = \mathbf{a} \times \mathbf{b}$. Note that $\{\mathbf{a}, \mathbf{b}, \mathbf{c}\}$ form a basis for \mathbb{R}^3 . Then, each point $\mathbf{x} \in \mathbb{R}^3$ can be written as follows:

¹https://www.youtube.com/watch?v=pydiO4PRjDw





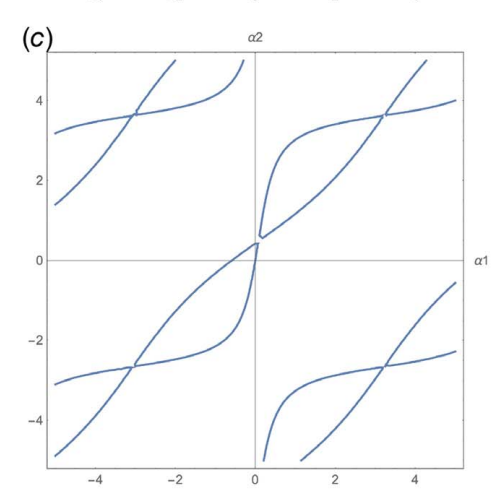


Fig. 5 The characteristics of the paths of motion depending on the relative sizes of ξ and δ : (a) $\delta < \xi$, (b) $\delta = \xi$, and (c) $\delta > \xi$

$$\mathbf{x} = k_a \mathbf{a} + k_b \mathbf{b} + k_c \mathbf{c}$$

where k_a , k_b , and k_c are a unique set of constants. We define $T_3^*(t): \mathbb{R}^3 \to \mathbb{R}^3$ by

$$T_3^*(t)\mathbf{x} = k_a T_1^*(t)\mathbf{a} + k_b T_2^*(t)\mathbf{b} + k_c [T_1^*(t)\mathbf{a} \times T_2^*(t)\mathbf{b}]$$

Theorem 1. T(t) defines a rigid motion.

Proof. To see that T(t) is well defined, first note that by construction, $T_1^*(t)$ and $T_2^*(t)$ are the identity on hinge lines H_1 and H_2 , respectively. Thus, the mapping T(t) is well defined on the points

of P_0 intersecting P_1 or P_2 . Next, we need to verify that $T_3^*(t)$ is consistent with $T_1^*(t)$ and $T_2^*(t)$ on hinge lines H_3 and H_4 , respectively. Note that:

(1) If $\mathbf{x} \in H_3$, then $\mathbf{x} = k_a \mathbf{a}$. Thus, $T_3^*(t)\mathbf{x} = k_a T_1^*(t)\mathbf{a} = T_1^*(t)(k_a \mathbf{a}) = T_1^*(t)\mathbf{x}$. Hence,

$$T_3^*(t)\mathbf{x} = T_1^*(t)\mathbf{x}$$

(2) If $\mathbf{x} \in H_2$, then $\mathbf{x} = k_b \mathbf{b}$. Thus, $T_3^*(t)\mathbf{x} = k_b T_2^*(t)\mathbf{b} = T_2^*(t)(k_b \mathbf{b}) = T_2^*(t)\mathbf{x}$. Hence,

$$T_3^*(t)\mathbf{x} = T_2^*(t)\mathbf{x}$$

Thus, we have the desired result. Therefore, T(t) is well defined. It is now clear from the definition of $T_3^*(t)$ and using the substitutions

$$T_3^*(t)\mathbf{a} = T_1^*(t)\mathbf{a}$$

$$T_3^*(t)\mathbf{b} = T_2(t)\mathbf{b}$$

$$T_3^*(t)\mathbf{c} = T_1^*(t)\mathbf{a} \times T_2^*(t)\mathbf{b}$$

that for $\mathbf{x} = k_a \mathbf{a} + k_b \mathbf{b} + k_c \mathbf{c} \in \mathbb{R}^3$

$$T_3^*(t)\mathbf{x} = k_a T_3^*(t)\mathbf{a} + k_b T_3^*(t)\mathbf{b} + k_c T_3^*(t)\mathbf{c}$$
 (15)

Using the identity given in Eq. (15), the fact that T_3^* is a linear transformation is a straightforward verification. In particular, for constants λ_1 and λ_2 and vectors,

$$\mathbf{x_1} = k_{a_1}\mathbf{a} + k_{b_1}\mathbf{b} + k_{c_1}\mathbf{c}$$
$$\mathbf{x_2} = k_{a_2}\mathbf{a} + k_{b_2}\mathbf{b} + k_{c_2}\mathbf{c}$$

we can immediately verify that

$$T_3^*(t)(\lambda_1\mathbf{x_1} + \lambda_2\mathbf{x_2}) = \lambda_1T_3^*(t)\mathbf{x_1} + \lambda_2T_3^*(t)\mathbf{x_2}$$

By construction, $T_1^*(t)$ and $T_2^*(t)$ are orthogonal transformations. To see that $T_3^*(t)$ is an orthogonal transformation, note that by design, the distance between $T_1^*(t)\mathbf{a}$ and $T_2^*(t)\mathbf{b}$ remains constant as t varies. Thus, for all t, the triangle with vertices $\mathbf{0}$, \mathbf{a} , and \mathbf{b} is congruent to the triangle with vertices $T(t)\mathbf{0}$, $T(t)\mathbf{a}$, and $T(t)\mathbf{b}$. Hence, $T_3^*(t)\mathbf{c} = T_1^*(t)\mathbf{a} \times T_2^*(t)\mathbf{b}$ has constant magnitude and is perpendicular to both T_1^* (t) \mathbf{a} and $T_2^*(t)\mathbf{b}$ throughout the motion. This means the tetrahedron with vertices $T_3^*(t)\mathbf{0}$, $T_3^*(t)\mathbf{a}$, $T_3^*(t)\mathbf{b}$, and $T_3^*(t)\mathbf{c}$. Thus, it must be the case that $T_3^*(t)$ is an orthogonal transformation. Therefore, T(t) defines a rigid motion.

Note that the aforementioned argument does not depend on \mathcal{C} being a circular cone, nor that \mathbf{a} and \mathbf{b} have the same z-coordinate. It is only required that $T_1^*(t)$ and $T_2^*(t)$ are orthogonal transforms and that the distance between $T_1^*(t)\mathbf{a}$ and $T_2^*(t)\mathbf{b}$ is constant throughout the motion. Thus, we can summarize these results by the following theorem.

THEOREM 2. Suppose \mathbb{C} is a generalized cone in \mathbb{R}^3 with cone point at $\mathbf{0}$ and a conical developable mechanism is constructed on \mathbb{C} , similarly as in Fig. 2, with hinge lines H_1 , H_2 , H_3 , and H_4 passing through the origin. Let \mathbf{a} and \mathbf{b} be points distinct from the origin on the hinge lines H_3 and H_4 , respectively. If there are linear transformation paths $T_1^*(t)$ and $T_2^*(t)$ acting on panels P_1 and P_2 , respectively, so that the distance between $T_1^*(t)\mathbf{a}$ and $T_2^*(t)$ \mathbf{b} are constant as t varies, then the motion defined by (14) is a rigid motion.

4 Observational Analysis

These results can be helpful in analyzing the behaviors of conical developable mechanisms that are particularly relevant for the use of these mechanisms in future applications. Identifying the location of bifurcation points is important, so that the motion can be adequately known and controlled. Determining whether a mechanism's motion is exclusively inside or outside of the reference cone is valuable for understanding which geometry is appropriate for use on solid surfaces (such as a rocket nose cone) to ensure that the mechanism's motion does not penetrate the surface. These concepts are discussed in this section.

Considering Fig. 5, note that in all cases there is a class of upward slanting curves, which represent motion in which α_1 and α_2 are increasing at nearly the same rate. We will refer to these curves as the \mathcal{E} -curves. The other curves we will refer to as the \mathcal{D} -curves. Note that the origin is contained in a \mathcal{D} -curve in each case.

The points where two motion curves intersect are called bifurcation points, and correspond to the change points of the mechanism. A bifurcation point represents a point in the motion in which there is more than one possible continuation of the motion, other than reversing the motion. For planar lamina emergent mechanisms, there must be a bifurcation point corresponding to when the mechanism is in its conformed position [15]. However, for this conical developable mechanism, the conformed position corresponds to the origin in the $\alpha_1\alpha_2$ -plane (i.e., $(\alpha_1, \alpha_2) = (0, 0)$), which is not a bifurcation point as illustrated in each case in Fig. 5. Indeed, bifurcation points occur at positions where the hinge lines lie in a single plane (see Ref. [4]). When $\delta \neq \xi$, in the conformed position, no three of the axes are coplanar. When $\delta = \xi$, in the conformed position, the axes for H_2 and H_3 coincide (consider Fig. 3 when $\delta = \xi$), but the four axes together are not coplanar. Further note that when $\delta = \xi$, if l is the axis containing H_2 and H_3 in the conformed position, then P_2 and P_3 , moving together, can rotate freely about l while holding l fixed, and hence holding P_1 fixed. Likewise, when the axes of H_1 and H_4 coincide, then P_1 and P_3 , moving together, can rotate freely about the axis containing H_1 and H_4 while holding P_2 fixed.

Consider again Fig. 5. When $\delta \neq \xi$, the bifurcation points arise only from the intersection of \mathcal{E} -curves with \mathcal{D} -curves. However, when $\delta = \xi$, bifurcation points may also arise from the intersection of \mathcal{D} -curves. We will refer to a bifurcation point that is the intersection of an \mathcal{E} -curve with a \mathcal{D} -curve as an *ordinary bifurcation point* and a bifurcation point that is the intersection of two \mathcal{D} -curves as an *extraordinary bifurcation point*. In particular, an extraordinary bifurcation point is the intersection of a horizontal and a vertical line in the motion path. Along a vertical line in the motion path, P_1 is fixed as P_2 moves freely. Along a horizontal line in the motion path, P_2 is fixed as P_1 moves freely.

To understand the transition of the shapes of the \mathcal{D} -curves as δ changes size in comparison to ξ , i.e., the transitions from Figs. 5(a) through 5(c), note that at $\delta = \xi$, the \mathcal{D} -curves have a stair-step pattern that, when pieced together differently, can be represented as a set of vertical and horizontal lines. Thus, the region of space near an extraordinary bifurcation point is divided into four quadrants. When δ decreases away from ξ , the \mathcal{D} -curves break into two continuous curves: one in the first quadrant and one in the third quadrant. Likewise, when δ increases away from ξ , the \mathcal{D} -curves break into two continuous curves: one in the second quadrant and one in the fourth quadrant.

4.1 Initial Motion. The compact nature of the conical developable mechanism is achieved when the mechanism is in its conformed position. As such, it is important to consider the initial motion as the mechanism moves from the conformed position. Greenwood described three behaviors (intramobility, extramobility, and transmobility) that characterize the motion of developable mechanisms as they move from their conformed position. For regular cylindrical [11] and conical [13] developable mechanisms, these behaviors can be predicted using graphical methods. We also note that as a change point mechanism, there are two possible configurations, open and crossed, and that the

conformed position represents a crossed configuration (see Ref. [15]).

We provide an analytical perspective for regular conical developable mechanisms. Note that if all panels start in the conformed position, the initial motion must be defined by a path that moves along a \mathcal{D} -curve. The initial direction of the \mathcal{D} -curve depends on the relative sizes of δ and ξ as follows:

- If $\delta < \xi$, we observe that when α_1 is initially increasing, then α_2 is initially decreasing (see Fig. 5(a)). Hence, if panel P_1 is initially moving outward, then panel P_2 must be initially moving inward, and vice versa. Greenwood et al. [11] refer to this type of behavior as *transmobile* (also see Ref. [19].)
- If $\delta = \xi$, recall that this is the case where H_2 and H_3 are colinear in the conformed position. Thus, panel P_1 must initially be kept fixed, while panel P_2 moves in either direction (see Fig. 5(b)).
- If δ>ξ, we observe that both panels initially move in the same direction, but P₁ moves at a slower rate than P₂ (see Fig. 5(c)). This behavior is called *intramobile* if the motion is toward the interior of the surface and *extramobile* if the motion is toward the exterior of the surface [11].
- **4.2 Bifurcation Points.** The characteristics of the possible continued motions at a bifurcation point also depends on the relative sizes of δ and ξ . The existence of the bifurcation points lead to unbounded motion paths in the $\alpha_1\alpha_2$ -plane.
 - If δ<ξ, at a bifurcation point, we observe that it is possible to move panels P₁ and P₂ in the same direction by continuing the motion along an ε-curve or in a different direction by continuing the motion along a D-curve. Each ε-curve intersects each D-curve at precisely one point and all bifurcation points connect to the origin. They form an array that is periodic in two directions.
 - If $\delta = \xi$, we observe that at an ordinary bifurcation point there is a choice to keep one panel, P_1 or P_2 , fixed while moving the other or to keep both panels in motion at nearly the same rate. At an extraordinary bifurcation point, only one panel can be put in motion while fixing the other, but either panel can be selected to be put in motion. In this case, all bifurcation points are connected to the origin. Both the set of ordinary bifurcation points and the set of extraordinary bifurcation points each form an array that is periodic in two direction.
 - If δ>ξ, we observe that both panels P₁ and P₂ must continue to move in the same direction. However, there are two possible rates at which this occurs. In this case, all bifurcation points are ordinary. There is a one-to-one correspondence between the ε-curves and D-curves that intersect. The set of bifurcation points connected to the origin is periodic in one direction. There are an infinite number of parallel sets.

Figure 6 illustrates positions of the conical developable mechanism corresponding to various points in the motion path when $\delta < \xi$. Recall that when $\delta < \xi$, we observe transmobile behavior. In particular, starting from the conformed position, the panels P_1 and P_2 must move in opposite directions, inward and outward, relative to the surface of the cone. Only in the case that $\delta > \xi$ is there a rigid motion that allows both of the panels to move in the same direction initially.

Note that, by design, our conical developable mechanism is a spherical parallelogram linkage, where the link angles of opposite links are equal. For modifications of our design that are not parallelogram linkages, see Ref. [13]. For these more generally designed mechanisms, the existence and types of bifurcation points in the motion will depend on whether they are Grashof mechanisms.

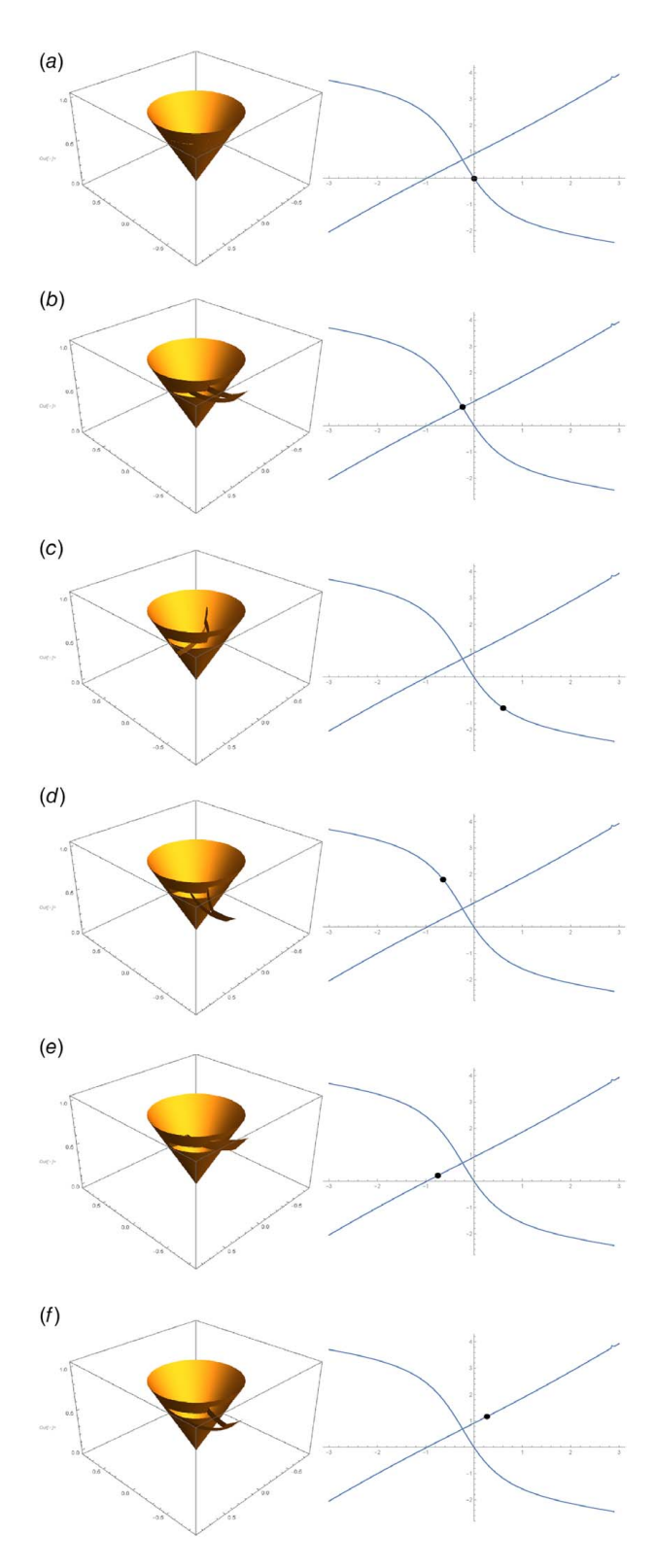


Fig. 6 Deflection at points of the motion path when $\delta < \xi$: (a) conformed position at $(\alpha_1, \ \alpha_2) = (0, \ 0)$, (b) coplanar hinge lines at bifurcation point, (c) along D-curve below bifurcation point, (d) along D-curve above bifurcation point, (e) along E-curve below bifurcation point, and (f) along E-curve above bifurcation point

5 Conclusion

In this article, we have demonstrated that conical developable mechanisms, as designed here, have rigid motion. We have also demonstrated how to analytically determine the motion and have provided a general description of the motion. The relationship between variables δ and ξ determines the motion of the mechanism with respect to the conical reference surface and predicts the behaviors (intramobile, extramobile, and transmobile) the mechanism can exhibit. The relative sizes of δ and ξ also determine the variety of bifurcation points that arise in the motion path. We have described how these bifurcation points arise and the behavior of the mechanism around the various types of bifurcation points. Furthermore, we proved that a conical four-bar mechanism constructed on a generalized cone has rigid motion provided that a motion can be found that preserves the distance between any two distinct points, one on each of the hinge lines H_3 and H_4 .

Funding Data

• National Science Foundation (NSF Grant No. 1663345.)

Conflict of Interest

There are no conflicts of interest.

Data Availability Statement

The authors attest that all data for this study are included in the paper.

References

- Fuchs, D., and Tabachnikov, S., 1999, "More on Paperfolding," Am. Math. Monthly, 106(1), pp. 27–35.
- [2] Stoker, J., 1969, Differential Geometry, Wiley-Interscience, New York.
- [3] Spivak, M. D., 1970, A Comprehensive Introduction to Differential Geometry, Publish or Perish, Inc., Houston, TX.
- [4] Nelson, T. G., Lang, R. J., Pehrson, N. A., Magleby, S. P., and Howell, L. L., 2016, "Facilitating Deployable Mechanisms and Structures Via Developable Lamina Emergent Arrays," ASME J. Mech. Rob., 8(3), p. 031006.
- [5] Pérez, F., and Suárez, J., 2007, "Quasi-Developable B-Spline Surfaces in Ship Hull Design," Computer Aided Design, 39(10), pp. 853–862.
- [6] Farmer, R. S., 1938, "Celestial Cartography," Publ. Astron. Soc. Pacific, 50(293), pp. 34–48.
- [7] Ceccato, C., 2012, "Material Articulation: Computing and Constructing Continuous Differentiation," Archit. Design, 82(2), pp. 96–103.
- [8] Wang, Y.-g., Wang, C.-h., Xiao, Y.-c., Chen, B., Zhou, S., Guo, J.-t., and Sun, M.-w., 2016, "Construction Methodology for Lip Surface of a Submerged Inlet," Aeros. Sci. Technol., 54, pp. 340–352.
- [9] Decaudin, P., Julius, D., Wither, J., Boissieux, L., Sheffer, A., and Cani, M.-P., 2006, "Virtual Garments: A Fully Geometric Approach for Clothing Design," Comput. Graphics Forum, 25(3), pp. 625–634.
- [10] Nelson, T. G., Zimmerman, T. K., Magleby, S. P., Lang, R. J., and Howell, L. L., 2019, "Developable Mechanisms on Developable Surfaces," Sci. Rob., 4(27), p. eaau5171.
- [11] Greenwood, J. R., Magleby, S. P., and Howell, L. L., 2019, "Developable Mechanisms on Regular Cylindrical Surfaces," Mech. Mach. Theory., 142, p. 103584.
- [12] Seymour, K., Sheffield, J., Magleby, S. P., and Howell, L. L., 2019, "Cylindrical Developable Mechanisms for Minimally Invasive Surgical Instruments," International Design Engineering Technical Conferences and Computers and Information in Engineering Conference, Anaheim, CA, Aug. 18, Vol. 59247, American Society of Mechanical Engineers, p. V05BT07A054.
- [13] Hyatt, L. P., Magleby, S. P., and Howell, L. L., 2020, "Developable Mechanisms on Right Conical Surfaces," Mech. Mach. Theory., **149**, p. 103813.
- [14] Shyu, T. C., Damasceno, P. F., Dodd, P. M., Lamoureux, A., Xu, L., Shlian, M., Shtein, M., Glotzer, S. C., and Kotov, N. A., 2015, "A Kirigami Approach to Engineering Elasticity in Nanocomposites Through Patterned Defects," Nat. Mater., 14(8), pp. 785–789.
- [15] Jacobsen, J. O., Winder, B. G., Howell, L. L., and Magleby, S. P., 2009, "Lamina Emergent Mechanisms and Their Basic Elements," ASME J. Mech. Rob., 2(1), p. 011003.
- [16] Grashof, F., 1883, Theoretische Maschinenlehre: Bd. Theorie Der Getriebe Und Der Mechanischen Messinstrumente, Vol. 2, L. Voss, Hamburg and Leipzig.
- [17] McCarthy, J. M., and Soh, G. S., 2010, Geometric Design of Linkages, Vol. 11, Springer Science & Business Media, New York.
- [18] Chiang, C., 1992, "Spherical Kinematics in Contrast to Planar Kinematics," Mech. Mach. Theory., 27(3), pp. 243–250.
- [19] Butler, J., Greenwood, J. R., Howell, L. L., and Magleby, S. P., 2021, "Limits of Extramobile and Intramobile Motion of Cylindrical Developable Mechanisms," ASME J. Mech. Rob., 13(6), p. 011024.